INVESTIGATION OF ISOTROPIC NON-NEWTONIAN FLUID TURBULENCE USING DIRECT NUMERICAL SIMULATION

Gary Fullerton and David McComb
Department of Physics and Astronomy
University of Edinburgh
James Clerk Maxwell Building
Mayfield Road
Edinburgh EH9 3JZ
United Kingdom

ABSTRACT

The particular non-Newtonian fluid under consideration is an incompressible dilute polymer solution. It has long been known experimentally that certain dilute polymer solutions may exhibit a significant reduction in turbulent drag (Ellis, 1970). Thus, understanding the behaviour of such fluids under turbulent conditions is of great importance. It is our aim to probe the basic dynamic properties of a dilute polymer solution, without any dependence on solid boundary conditions. Our approach is to study different non-Newtonian equations, corresponding to different polymer solution models, via the direct numerical simulation of homogeneous isotropic turbulence. In this way we have identified changes within the structure of turbulence itself which may be related to the 'drag reduction' phenomenon.

INTRODUCTION

The study of non-Newtonian fluids is a large and varied field due to the myriad of possible fluid types which may be produced. The prediction of the behaviour of such fluids is obviously of immense importance because of their numerous industrial applications. However these fluids also generate a great deal of interest simply because they may exhibit complex, often counter intuitive, behaviour compared to that of a Newtonian fluid. At Edinburgh we have focused our attention on identifying the differences in turbulent structure and statistics between Newtonian solvents and dilute polymer solutions. It has been found that by dissolving a small amount of long-chain polymers ($\sim 4\%$ concentration) in a Newtonian solvent the mean flow rate within a pipe or channel may be increased by 50-70% for equal pressure gradients (McComb & Rabie, 1982), without the physical nature of the fluid being drastically altered.

A substantial amount of experimental research has gone into examining dilute polymer solutions mainly due to their 'drag reducing' properties, which were first discovered by Toms, (1949). Recent developments in computing have resulted in machines powerful enough to simulate such flows with Taylor-Reynolds numbers high enough to form some qualitative agreement with experimental observations. Hence the trend, to date, has been to perform computational simulations of dilute polymer solutions within specific flow domains, such as turbulent channel or pipe flows.

Since we are interested in identifying the alterations within the turbulent dynamics produced by the presence of these polymers alone, we have opted to simulate our solution within a infinitely repeating cube subject to periodic boundary conditions. The direct numerical simulation (DNS) of a Newtonian solvent in such a domain is a well established and standard technique. We begin by outlining our general approach to non-Newtonian turbulence, and then specify the particular polymer models chosen.

NON-NEWTONIAN TURBULENCE

Any incompressible fluid will obey the momentum and mass conservation equations,

$$\rho Du_\alpha(\mathbf{x},t)/Dt = -\partial p(\mathbf{x},t)/\partial x_\alpha + \partial \tau_{\alpha\beta}(\mathbf{x},t)/\partial x_\beta, \quad (1)$$

$$\partial u_\alpha(\mathbf{x},t)/\partial x_\alpha = 0, \quad (2)$$

where ρ represents the density per unit mass, $u_\alpha(\mathbf{x},t)$ the velocity and $p(\mathbf{x},t)$ the pressure. When dealing with non-Newtonian turbulence the total deviatoric stress of the solution, $\tau_{\alpha\beta}(\mathbf{x},t)$, is split into two parts, namely the Newtonian and the polymer contributions,

$$\tau_{\alpha\beta}(\mathbf{x},t) = \tau^N_{\alpha\beta}(\mathbf{x},t) + \rho\tau^P_{\alpha\beta}(\mathbf{x},t), \quad (3)$$

where $\tau^P_{\alpha\beta}(\mathbf{x},t)$ is assumed to be in kinematic form. For the Newtonian part we have,

$$\tau^N_{\alpha\beta}(\mathbf{x},t) = 2\rho\nu_0 e_{\alpha\beta}(\mathbf{x},t), \quad (4)$$

where ν_0 is the kinematic viscosity of the Newtonian solvent and $e_{\alpha\beta}(\mathbf{x},t)$ is the rate of strain tensor. If we then Fourier transform the momentum conservation equation and eliminate the pressure term via the incompressibility condition, equation (2), it is easily shown that in wavenumber ($\mathbf{k}$) space we then have the equation,

$$(\partial_t + \nu_0 k^2)u_\alpha(\mathbf{k},t) = M_{\alpha\beta\gamma}(\mathbf{k})\Big[\int d^3j\, u_\beta(\mathbf{j},t)u_\gamma(\mathbf{k}-\mathbf{j},t) - \tau^P_{\beta\gamma}(\mathbf{k},t)\Big], \quad (5)$$

where,

$$M_{\alpha\beta\gamma}(\mathbf{k}) = (2i)^{-1}[k_\beta D_{\alpha\gamma}(\mathbf{k}) + k_\gamma D_{\alpha\beta}(\mathbf{k})] \quad (6)$$

and the isotropic projector $D_{\alpha\beta}(\mathbf{k})$ is expressed as

$$D_{\alpha\beta}(\mathbf{k}) = \delta_{\alpha\beta} - k_\alpha k_\beta |\mathbf{k}|^{-2} \quad (7)$$

From equation (5) it is possible to model a non-Newtonian solution provided we have an expression for the polymer stress. Note that if the polymer stress contribution is zero we regain the Navier-Stokes equations.

Since long-chain polymers are made from many individual monomer segments, they have a very complicated internal motion. To model the motion of the polymers within a fully turbulent fluid, in all their complexity, would be far too demanding computationally, hence we must seek approximations which mimic the effect the polymers have on the fluid. Below we discuss the range of models which we have implemented.

Viscous Increase Model

The concept behind the viscous increase model (VIM) is very simple and is based on two factors. Firstly, the size of the polymers will be small compared to the general scale of the flow and so we assume that any change in the turbulent dynamics of the fluid due to polymer interactions will only occur at small scales. Secondly, the polymer interactions will result in an increase in the viscosity of the fluid. This is a plausible assumption as experimental measurements show that the extensional viscosity of dilute polymer solutions can be several orders of magnitude greater than that of the Newtonian solvent, (Metzner & Metzner, 1970).

Thus, we chose a non-Newtonian model with a coefficient of viscosity which differed from the Newtonian only at small scales. Such a fluid can be modeled by having a polymer stress contribution given by,

$$\tau^P_{\alpha\beta}(\mathbf{k},t) = 2\nu(k)e_{\alpha\beta}(\mathbf{k},t), \quad (8)$$

where the viscosity of the solution is now a scalar function of the wavenumber magnitude. The actual form of the viscosity function is given by,

$$\nu(k) = \begin{cases} 0 & : \ k \le k_a \\ \nu_s(k) & : \ k_a < k < k_b \\ (\lambda_\nu - 1)\nu_0 & : \ k \ge k_b \end{cases} \quad (9)$$

where $\lambda_\nu > 1$ and $\nu_s(k)$ interpolates between the two constant values. For simplicity we chose $\nu_s(k)$ such that the viscosity is increased at a constant rate over the local wavenumber band $k_a < k < k_b$. Figure 1 shows a graphical representation of the total viscosity of the fluid. For our calculations we chose $\lambda_\nu = 2.5$ with $k_a = 60\%$ and $k_b = 80\%$ of the maximum wavenumber simulated.

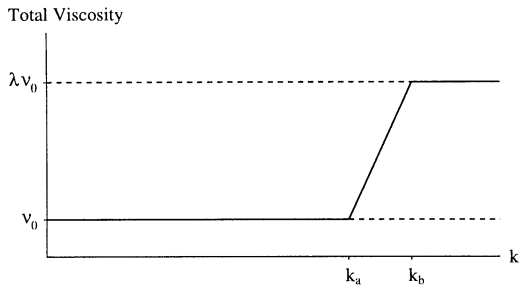

Figure 1: Graphical representation of the wavenumber space viscosity of the VIM fluid.

Note that realistically the size of the polymers are such that the scales on which they directly interact with the turbulence would correspond to a wavenumber region far higher than is possible to reach with current numerical simulations. However the investigation of the VIM is not without rewards as will be discussed later.

Aligned Polymer Model

The aligned polymer model (APM) is a step closer to a more realistic polymer model. Instead of explicitly perturbing the scales of the flow as with the VIM, here we incorporate a polymer stress term which is based on the actual motion of the polymers within the turbulent fluid. The APM assumes that the length of the polymers remain constant and that their motion can be represented by an embedded unit vector field, $n_\alpha(\mathbf{x},t)$, giving their directional orientations. The full equations of motion for such a coupled vector field are given by Hinch and Leal, (1973), and they ultimately lead to a macroscopic polymer stress contribution which is dependent on an ensemble average of the dyadic product of the polymer orientations, $\langle n_\alpha(\mathbf{x},t)n_\beta(\mathbf{x},t)\rangle$.

These equations can be simplified by assuming that, on average, the polymers will align with the instantaneous velocity field of the fluid. The justification for this approximation follows from experimental observations that high aspect ratio particles tend to align with the flow direction, (Stover *et. al.*, 1992). A further simplification may be made by comparing the equations of motion in specific flows (such as steady simple shear flow) to experimental data for dilute polymer solutions and adjusting the model parameters accordingly. In this way it has been shown that the APM polymer stress contribution may be expressed as, (den Toonder, 1995),

$$\tau^P_{\alpha\beta}(\mathbf{x},t) = \nu_1 e_{\sigma\gamma}(\mathbf{x},t)\frac{u_\sigma(\mathbf{x},t)u_\gamma(\mathbf{x},t)}{u(\mathbf{x},t)^2}\frac{u_\alpha(\mathbf{x},t)u_\beta(\mathbf{x},t)}{u(\mathbf{x},t)^2} \quad (10)$$

where ν_1 is a material constant which depends on the solvent viscosity and the polymer concentration. Since this particular non-Newtonian fluid has a directional element at each material point, along with viscous effects

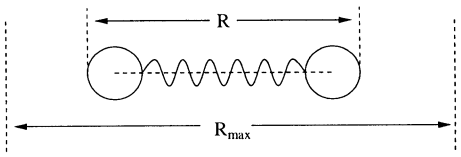

Figure 2: The bead-spring polymer representation of a FENE Polymer model. For the FENE-P representation the two end beads are connected by a non-linear spring, such that the spring force tends to infinity as $\langle R^2 \rangle \to R^2_{\max}$.

we also expect it to exhibit localised anisotropic properties. We chose $\nu_1 = 17\nu_0$, which corresponds to uniaxial and biaxial viscosities of $20\nu_0$ and $14.5\nu_0$ respectively.

FENE-P Polymer Model

Our third and final model is the finitely extensible, non-linear, elastic dumbbell, with the Peterlin approximation (FENE-P). For a FENE-P fluid we model the long-chain polymer as a simple bead-spring dumbbell as shown in Figure 2. The force in the connector between the two beads of a polymer at a particular material point is given by a non-linear spring force,

$$f\left(\langle R^2 \rangle\right) = H\left[1 - \frac{\langle R^2 \rangle}{R^2_{\max}}\right]^{-1} = HZ, \qquad (11)$$

where H is a constant, R is the length of the polymer and $R_{\max}$ is the maximum length. Hence the spring force tends to infinity as $\langle R^2 \rangle \to R^2_{\max}$. The derivation of the FENE-P model may be found in Wedgewood and Bird (1988), here we only highlight the salient features.

The FENE-P model is similar to the APM, in that we represent the motion of the polymers by a vector field $R_\alpha(\mathbf{x}, t)$, giving their length and orientation at each material point. Again the macroscopic polymer stress contribution is a function of the ensemble averaged dyadic products of the vector field $\langle R_\alpha(\mathbf{x}, t) R_\beta(\mathbf{x}, t) \rangle$ and is given by,

$$\tau^P_{\alpha\beta}(\mathbf{x}, t) = \frac{nk_BT}{\rho}\left(Z(\mathbf{x}, t)A_{\alpha\beta}(\mathbf{x}, t) - \delta_{\alpha\beta}\right), \qquad (12)$$

where n is the number density, k_B the Boltzmann constant and T the temperature. The dimensionless quantities in equation (12) are,

$$A_{\alpha\beta}(\mathbf{x}, t) = \frac{H}{k_BT}\langle R_\alpha(\mathbf{x}, t) R_\beta(\mathbf{x}, t) \rangle \qquad (13)$$

and

$$Z(\mathbf{x}, t) = [1 - (1/b)A_{\alpha\alpha}(\mathbf{x}, t)]^{-1}. \qquad (14)$$

Hence to calculate the polymer stress we must obtain $A_{\alpha\beta}(\mathbf{x}, t)$. We do this by solving the evolution equation below,

$$\begin{aligned} &\lambda_H D A_{\alpha\beta}(\mathbf{x}, t)/Dt \\ &\quad = L_{\alpha\sigma}(\mathbf{x}, t)A_{\sigma\beta}(\mathbf{x}, t) + L_{\beta\sigma}(\mathbf{x}, t)A_{\sigma\alpha}(\mathbf{x}, t) \\ &\quad -Z(\mathbf{x}, t)A_{\alpha\beta}(\mathbf{x}, t) + \delta_{\alpha\beta}, \end{aligned} \qquad (15)$$

where the constant, λ_H, is the relaxation time of the polymers and $L_{\alpha\beta}(\mathbf{x}, t)$ is the deformation gradient.

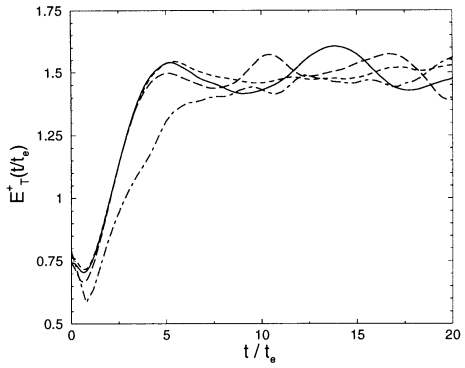

Figure 3: Evolution of the total energy, (——) Newtonian, (-----) VIM, (– – –) APM and (–·–) FENE-P. A statistically stationary state evolves after $\sim$ 5 eddy turnovers. Total energy

The dimensionless constant appearing in equation (14) represents the maximum extension, $b = HR^2_{\max}/k_BT$, and so we have the condition $A_{\alpha\alpha}(\mathbf{x}, t) < b$. For our FENE-P calculations we chose $b = 50$, and $nk_BT\lambda_H/\rho$ such that the ratio of the solvent viscosity to total zero-shear rate solution viscosity, $\beta = 0.5$. The viscoelastic flow is characterized by the dimensionless Weissenberg number, $We = \lambda_H \times e$, where e is the magnitude of the rate of strain tensor.

Although this model is more complicated than the VIM or the APM it is still a rather crude approximation to a long-chain polymer. However it does embody the orientational and viscoelastic nature of a dilute polymer solution.

NUMERICAL PROCEDURE

For our DNS calculations we followed the spectral method originally devised by Orszag (1969) for Newtonian fluids. The velocity field in wavenumber space is integrated forward in time via a second order Runge-Kutta algorithm. The same procedure was used for the non-Newtonian models with the only modification to the algorithm being the calculation of the polymer stresses. All terms in the equations which resulted in wavenumber space convolutions were accordingly calculated as products in real space to reduce the computational workload. We performed partial dealiasing by the random shifting method (Rogallo, 1981) and truncation at $\sqrt{2}/3\ N$, where N was the grid resolution.

For the FENE-P fluid in particular we note that the equations of motion are known to be unstable numerically. The addition of a small stress diffusivity term, $\kappa\nabla^2 A_{\alpha\beta}(\mathbf{x}, t)$, $\kappa \ll 1$, in equation (15) was required to stabilize the simulation. This procedure was proposed and investigated by Sureshkumar and Beris (1995), who showed that the presence of a small diffusivity term will not affect the general dynamics of the system, but will increase the stability of the numerics.

Our numerical simulations were all performed on a 512-processor Cray T3D parallel machine with 64 Mb of memory per processor.

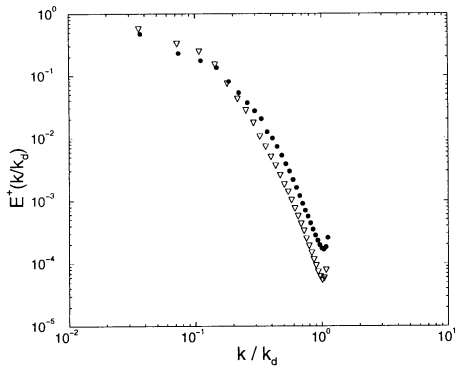

Figure 4: Time averaged energy spectra for Newtonian (•) and FENE-P (▽) fluids. Energy spectra for VIM and APM show similar reduction in energy at high wavenumber modes.

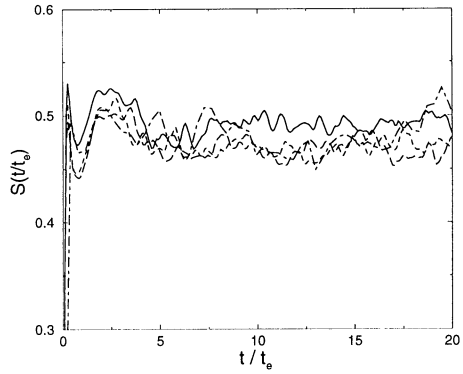

Figure 5: The skewness factor, $S(t/t_e)$, of the velocity distributions (——) Newtonian, (-----) VIM, (– – –) APM and (–·–) FENE-P. We observe, on average, a reduction in $S(t/t_e)$ for the non-Newtonian fluids.

RESULTS

In this section we present results from spectral simulations of statistically stationary turbulence on a 64^3 grid. We are currently repeating this work on a 128^3 grid, the results of which we intend to present at the conference. We are restricted to such low resolutions due to the additional computational cost of calculating the polymer stress term. For example, at 128^3 resolution the FENE-P model requires 0.2 CPU-Hours per timestep compared to 0.05 CPU-Hours per timestep for the Newtonian simulation.

For ease of comparison, each simulation was performed with the same initial conditions and solvent viscosity, ν_0. The energy and timescales depicted are non-dimensionalised via the square of the time averaged rms velocity, and the eddy turnover time, respectively. To avoid any anomalous values the time averaging was performed only after the statistically steady state had evolved.

We achieved a statistically stationary turbulent regime by implementing a low wavenumber forcing

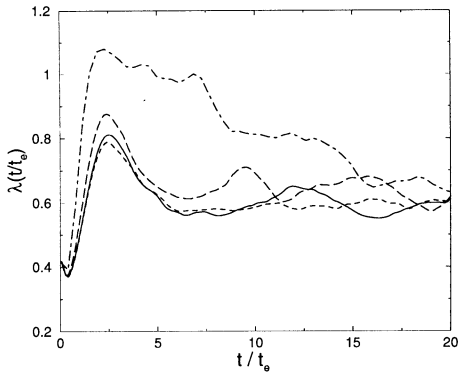

Figure 6: The Taylor microscale $\lambda(t/t_e)$, (——) Newtonian, (-----) VIM, (– – –) APM and (–·–) FENE-P. This represents an approximation to the spatial correlation length within the fluid. $\lambda(t/t_e)$ generally appears to be higher for the non-Newtonian fluids, with a marked increase observed for the FENE-P.

scheme which results in a constant energy input rate, as detailed in McComb *et. al* (1997). Figure 3 shows the time evolution of the total energy where it can clearly be seen that a steady state was reached after approximately 5 eddy turnovers. The simulations had a Taylor-Reynolds value, $R_\lambda \sim 80$ and for the FENE-P, $We \sim 3.5$ and $\langle A_{\alpha\alpha}(\mathbf{x},t)\rangle \sim 0.7b$. An important indication of the turbulent dynamics is given by the energy spectrum. This was calculated by means of a shell averaging technique in wavenumber space. For isotropic systems this is equivalent to performing ensemble averages over many realizations. However for this approach to be valid we must ascertain whether our non-Newtonian fluids are indeed isotropic. We employed a similar method to that of Curry *et. al.* (1984), and it was found that for each simulation the isotropy factor, I, fluctuated by a few percent around a value of 1, hence we conclude our simulations were close enough to 'perfect isotropy', $I = 1$, for shell averaging to be valid in all cases.

In Figure 4 we plot a comparison between the time averaged energy spectra of the FENE-P model and that of the Newtonian simulation. We note that qualitatively, the spectra for the VIM and APM (not plotted) are very similar to that of the FENE-P. The non-Newtonian fluids all exhibit a steeper gradient with an energy decrease at high wavenumbers and a slight increase in energy at lower wavenumber modes, compared to the Newtonian case. It is interesting to note that the energy decrease in the VIM fluid was over a range of scales outwith the localised wavenumber band where the polymer stress term is non-zero. This result highlights the strongly non-local nature of turbulence in general in that a relatively small increase in the viscosity (λ_ν) at high wavenumbers will alter the dynamics of the flow over all scales. The spectra displayed in Figure 4 are similar in character to those found experimentally in dilute polymer solutions (McComb & Rabie, 1982) and more recently for drag reducing surfactant suspensions, (Schmidt *et. al.*, 1999).

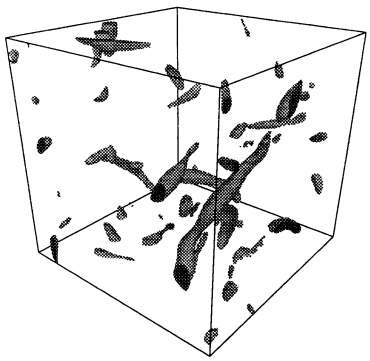

Figure 7: Iso-surface plots of the vorticity for the Newtonian fluid at 20 t/t_e. The magnitude of vorticity plotted are for a value of 60% of the maximum vorticity.

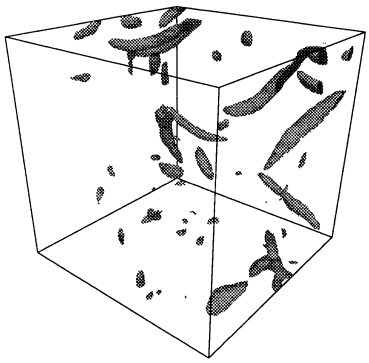

Figure 8: Iso-surface plots of the vorticity for the VIM fluid at 20 t/t_e. The magnitude of vorticity plotted are for a value of 60% of the maximum vorticity.

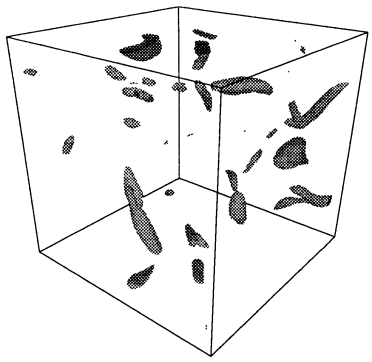

Figure 9: Iso-surface plots of the vorticity for the APM fluid at 20 t/t_e. The magnitude of vorticity plotted are for a value of 60% of the maximum vorticity.

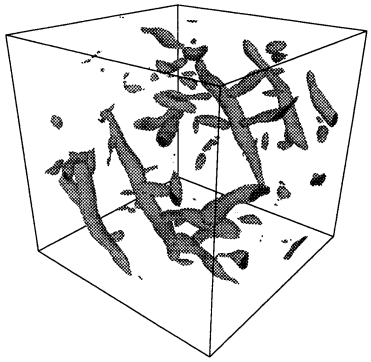

Figure 10: Iso-surface plots of the vorticity for the FENE-P fluid at 20 t/t_e. The magnitude of vorticity plotted are for a value of 60% of the maximum vorticity.

The skewness factor of the velocity derivative distribution is representative of the average energy transfer efficiency from low to high wavenumber modes. Again the VIM, APM and FENE-P models all display similar characteristics, with a reduction in the skewness factor for each compared to that of the Newtonian as illustrated in Figure 5. This drop in energy transfer efficiency is consistent with the energy spectra results. In which more energy appears to be present within the lower wavenumber modes.

Another clue as to the changes in turbulent structure of the non-Newtonian models may be found in the value of the Taylor microscale, $\lambda(t/t_e)$. This can be thought of as an approximate indicator of the spatial correlation length within the fluid. Figure 6 shows the evolution of $\lambda(t/t_e)$ for each simulation, we observe an increase for all non-Newtonian models with a marked increase in correlation for the FENE-P model. Since the VIM and APM represent viscous and anisotropic properties, we may attribute this large deviation from the other models to the elastic properties of the FENE-P.

To further investigate the turbulent structures it is helpful to examine three dimensional iso-surface plots of vorticity magnitudes. These are illustrated in Figures 7 - 10, for each fluid. The iso-surface plots display the evolved vorticity fields after 20 eddy turnover times and so are representative of the fully turbulent, statistically stationary state. By viewing several such vorticity plots we see that, in general, the non-Newtonian fluids all display longer vorticity structures compared to that of the Newtonian fluid. This is consistent with the earlier Taylor microscale results which indicated a longer spatial correlation length. Also by increasing the magnitude of the iso-surfaces of vorticity plotted, it was found that the presence of these structures declined more rapidly than in the Newtonian case. These results bear some resemblance to the experimental observations where small scale structure has been sup-

pressed by drag reducing polymer additives, (McComb *et. al.*, 1977).

Here we have plotted the iso-surfaces of vorticity with the magnitude at a value of 60% of the maximum. This value was chosen as we still observe distinct differences in structure between Newtonian and non-Newtonian fluids. However, it is also possible to notice differences between the non-elastic VIM and APM fluids and that of the FENE-P.

It is interesting to compare the FENE-P model (Figure 10) to that of the APM (Figure 9). Although the average polymer length remains almost constant the FENE-P exhibits a vastly different vorticity structure to that of the APM. The average length of the FENE-P vorticity structures are almost double that of the APM and seem to readily exist in close vortex pairs. Since the the average polymer length remains almost constant we can attribute this to localized elastic properties of the FENE-P.

CONCLUSIONS

From the range of model types implemented it was found that the statistical results from the VIM, APM and the FENE-P were similar, albeit in a qualitative sense. Each model displayed characteristics which are apparent in actual drag reducing dilute polymer solutions, such as the attenuation of the energy spectrum at high wavenumbers and the reduction of small scale structure. The presence of the polymer additives appear to reduce the energy transfer efficiency of the solution, resulting in more energy being contained within the lower wavenumber modes. Consequently larger vortex structures appear within the flow. This seems to be similar to a proposed mechanism for drag reduction in channel flow outlined in Dimitropoulous *et. al.*, (1998) whereby the presence of wider wall eddies are thought to be responsible for the observed drag reduction.

From the VIM and APM simulations we can conclude that increased viscous actions and the presence of localised anisotropic properties demonstrated by dilute polymer solutions have an important role in the drag reduction process. Although these conclusions have been reached before, (den Toonder, 1995) we have discovered that these properties are inherent in isotropic turbulence and are not restricted directional flows with solid boundary conditions.

Finally, from the iso-surface vorticity plots, we conclude that to accurately model a polymer with elastic properties, we must take account of the localized elastic nature of the flow, otherwise the resulting dynamics of the solution will be significantly different.

At the conference we intend to present similar results but implemented on a 128^3 grid, this should give a higher Taylor-Reynolds number and a larger range of wavenumbers. Hence we expect to find similar but more pronounced effects. We also hope to investigate decaying turbulence as we may find certain features of the turbulent behaviour of these non-Newtonian fluids that are unobservable during steady state simulations.

ACKNOWLEDGEMENTS

Computing facilities were provided by the Edinburgh Parallel Computing Centre. G.F. would like to acknowledge the financial support of the Scottish International Education Trust and of the Engineering and Physical Sciences Research Council.

REFERENCES

Curry, J.H., Herring, J.R., Loncaric, J. and Orszag, S., 1984, "Order and disorder in two- and three-dimensional Bérnard convection," *J. Fluid Mech.*, Vol. 147, pp. 1 – 38.

Dimitropoulous, C.D., Sureshkumar, R. and Beris, A.N., (1998), "Direct numerical simulation of viscoelastic turbulent channel flow exhibiting drag reduction: effect of the variation of rheological parameters," *J. Non-Newtonian Fluid Mech.*, Vol. 79, pp. 433 – 468.

Ellis, E.D., 1970, "Effects of shear treatment on drag reducing polymer solutions and fibre suspensions," *Nature*, Vol. 226, pp. 352 – 353.

Hinch, E.J. and Leal L.G., 1973, "Time-dependent shear flows of a suspension of particles with weak Brownian rotations," *J. Fluid Mech.*, Vol. 57, pp. 753 – 767.

McComb, W.D., Allan, J. and Greated, C.A., 1977, "Effect of polymer additives on the small scale structure of grid generated turbulence," *Phys. Fluids*, Vol. 292, pp. 873 – 979.

McComb, W.D. and Rabie L. H., 1982, "Local drag reduction due to injection of polymer solutions into turbulent flow in a pipe," *AIChE Journal*, Vol. 28, No. 4, pp. 547 – 565.

McComb, W.D., Yang, T.-J., Young, A.J. and Machiels, L., 1997, "Investigation of renormalization group methods for the numerical simulation of isotropic turbulence," *Proc. 11th Symp. on Turbulent Shear Flows*, Grenoble, pp. 4-23 – 4-27.

Metzner, A.B. and Metzner, A.P., 1970, "Stress levels in rapid extensional flows of polymeric fluids," *Rheol. Acta*, Vol. 9, pp. 174 – 181.

Orszag, S., 1969, "Numerical methods for the simulation of turbulence," *Phys. Fluids (suppl. 2)*, Vol. 12, pp. 250 – 257.

Rogallo, R.S., 1981, "Numerical experiments in homogeneous turbulence," NASA TM-81315.

Schmidt, G.M., Warholic, M.D. and Hanratty, T.J., 1999, "The influence of a drag reducing surfactant on a turbulent velocity field," *To be published.*

Stover, C.A., Koch, D.L. and Cohen, C., 1992, "Observations of fibre orientation in simple shear flow of semi-dilute suspensions," *J. Fluid Mech.*, Vol. 238, pp. 277 – 296.

Sureshkumar, R. and Beris, A.N., 1995, "Effect of artificial stress diffusivity on the stability of numerical calculations and the flow dynamics of time-dependent viscoelastic flows," *J. Non-Newtonian Fluid Mech.*, Vol. 60, pp. 53 – 80.

Toms, B.A., 1949, "Some observations on the flow of linear polymer solutions through straight tubes at large Reynolds numbers," *Proc. 1st Int. Congress Rheol.*, North Holland, pp. II 135 – 141.

den Toonder, J.M.J., 1995, "Drag reduction by polymer additives in a turbulent pipe flow: Laboratory and numerical experiments," *PhD Thesis, Technische Universiteit Delft.*

Wedgewood, L.E. and Bird, R.B., 1988, "From molecular models to the solution of flow problems," *Ind. Eng. Chem. Res.*, Vol. 27, pp. 1313 – 1320.